Supporting Information

Diversified AIE and mechanochromic luminescence based on carbazole derivatives decorated dicyanovinyl groups: Effects of Substitution Site and Molecular Packing

Kai Wang, [‡,†] Hui Xiao,[‡,†] Li Qian,[†] Mingxi Han,[†] Xianfeng Wu,[†] Zhiyong Guo,[*,†,§] and Hongbing Zhan[*,†]

[†]College of Materials Science and Engineering, Fuzhou University, Fuzhou 350108, Fujian, PR China

[§]Key Laboratory of Eco-materials Advanced Technology, Fuzhou University, Fujian Province, PR China

* Corresponding authors.

E-mail address: guozhy@fzu.edu.cn (Zhiyong Guo) and hbzhan@fzu.edu.cn (Hongbing Zhan)

Table of contents

Section 1. FTIR spectra

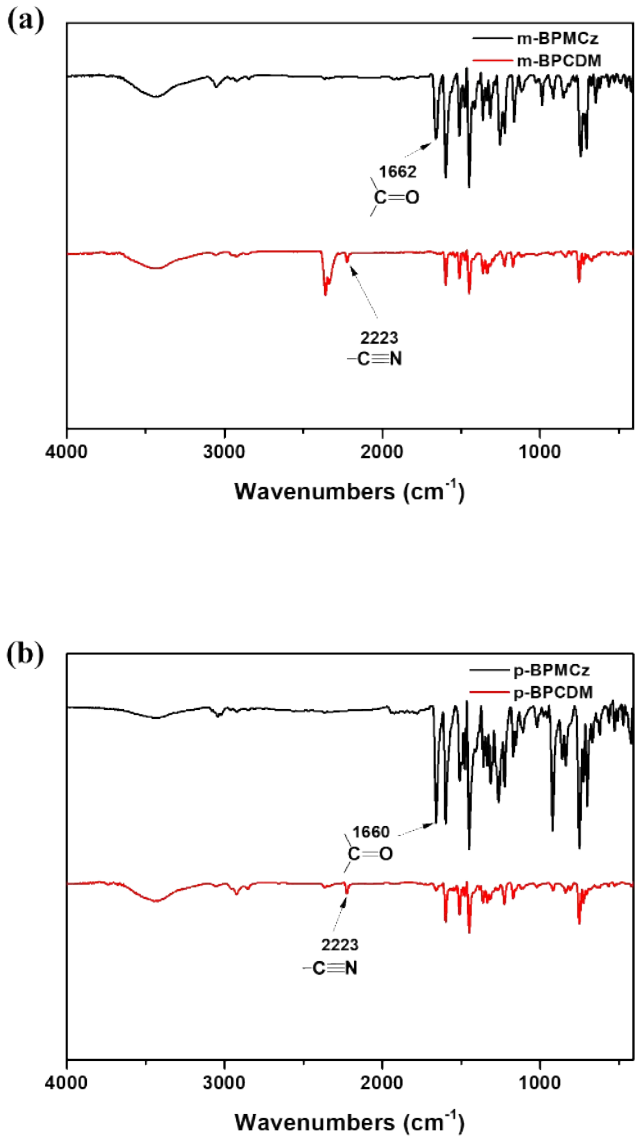

Fig. S1 (a) FTIR spectrum of m-BPMCz and m-BPCDM. (b) FTIR spectrum of p- BPMCz and p-BPCDM.

Section 2. NMR Spectra

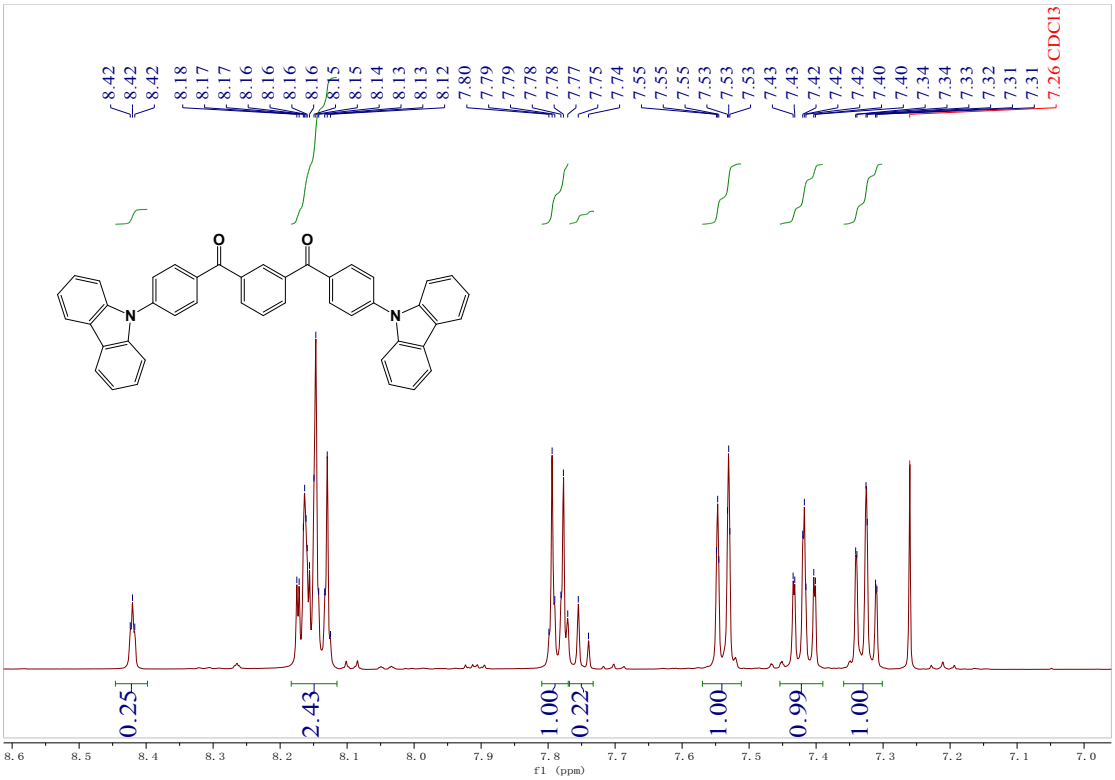

Fig. S2 ^{1}H NMR spectrum of m-BPMCz in $CDCl_3$.

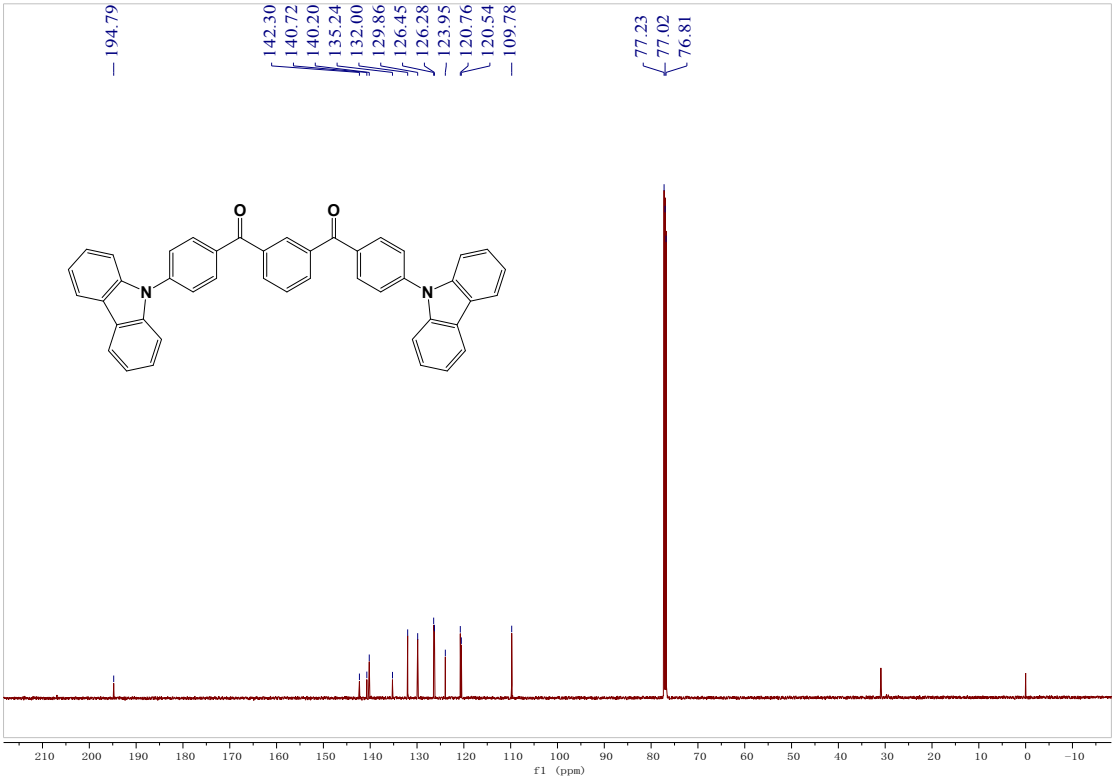

Fig. S3 ^{13}C NMR spectrum of m-BPMCz in $CDCl_3$.

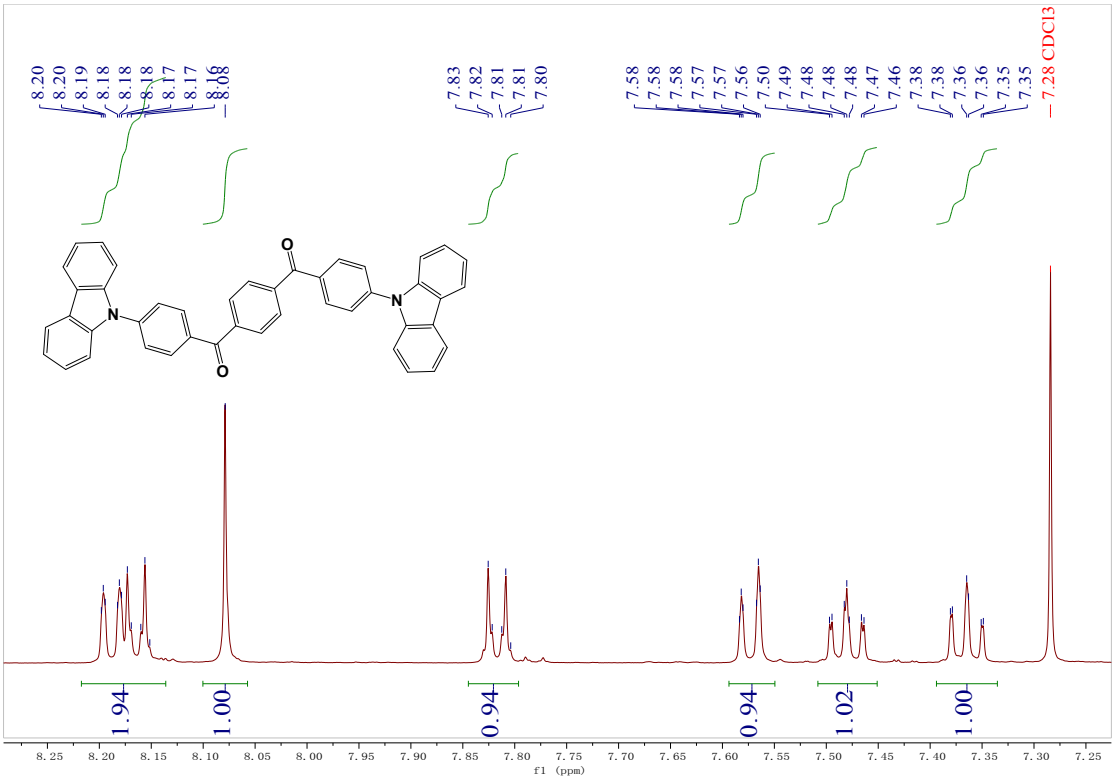

Fig. S4 ^{1}H NMR spectrum of p-BPMCz in $CDCl_3$.

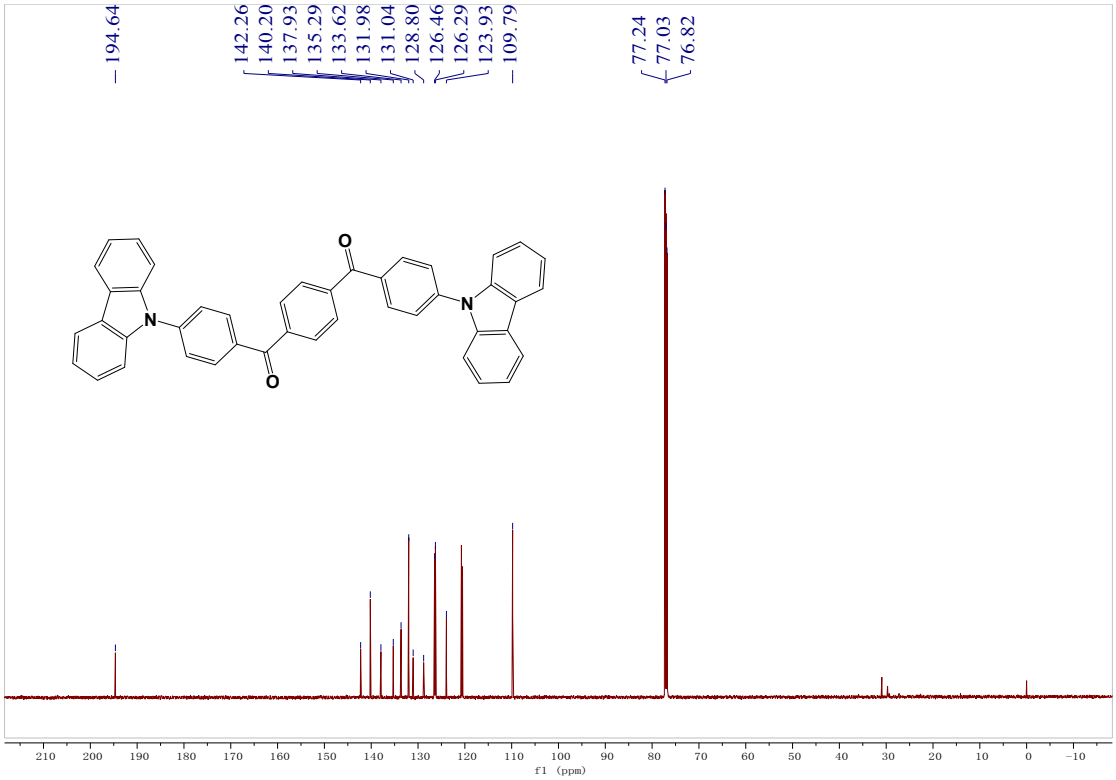

Fig. S5 ^{13}C NMR spectrum of p-BPMCz in $CDCl_3$..

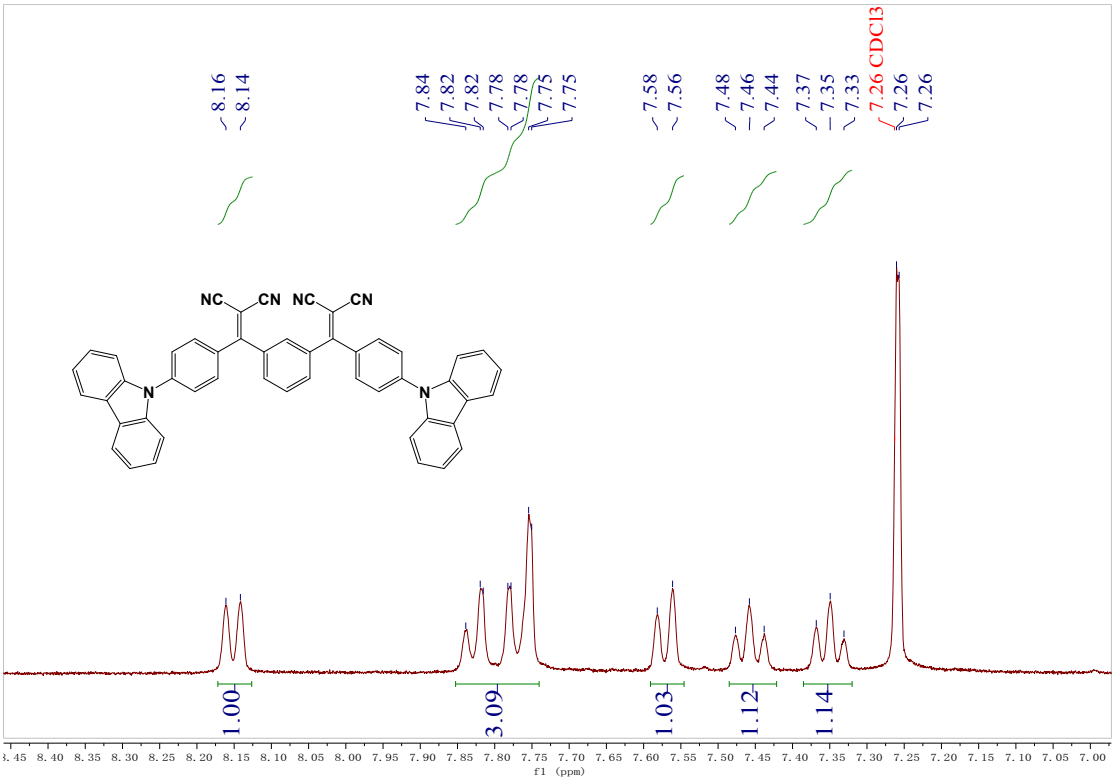

Fig. S6 ^{1}H NMR spectrum of m-BPCDM in $CDCl_3$.

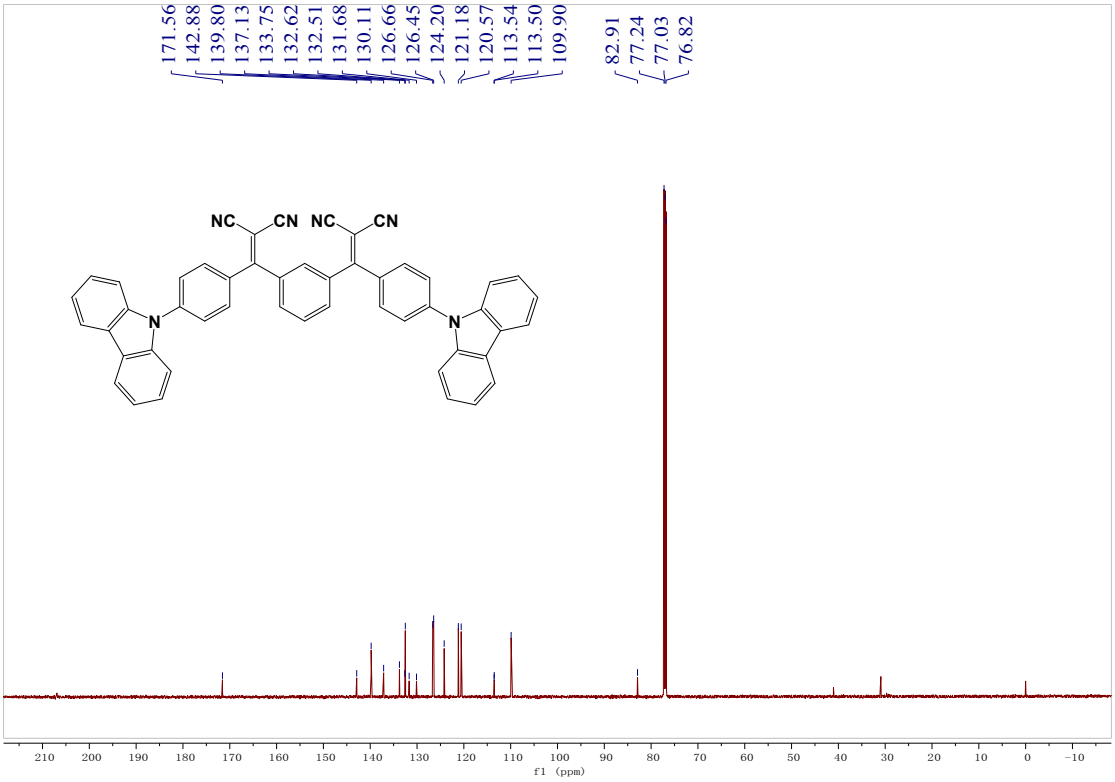

Fig. S7 ^{13}C NMR spectrum of m-BPCDM in $CDCl_3$.

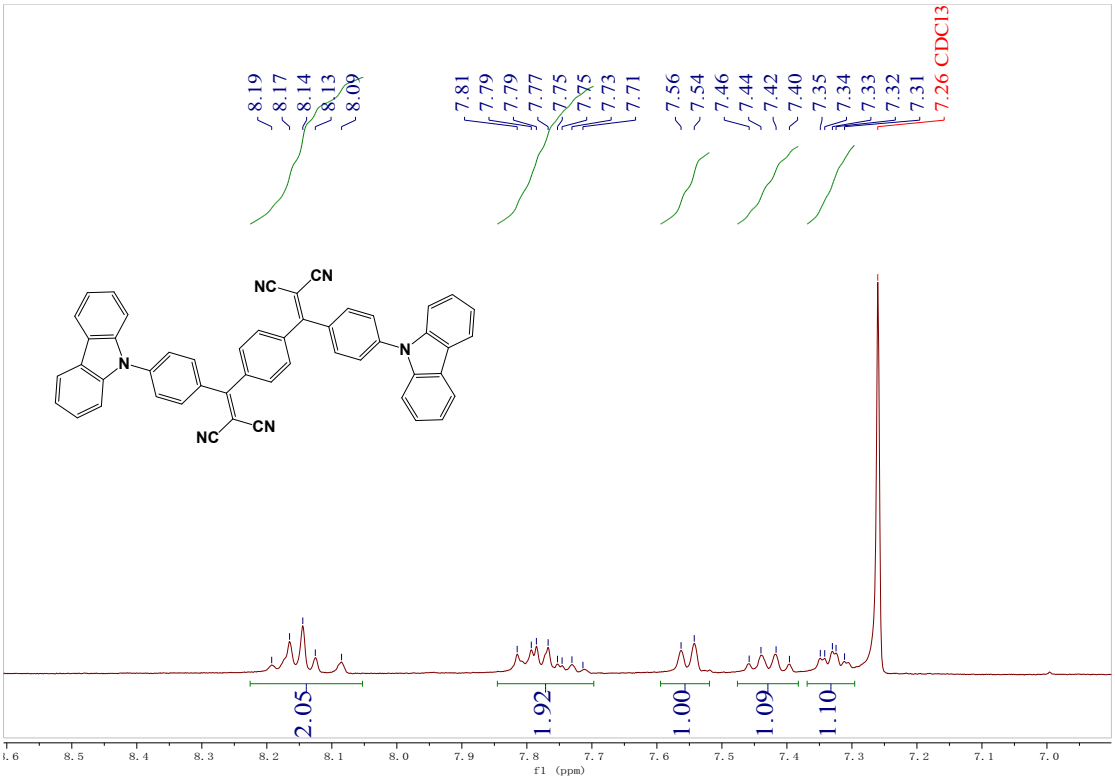

Fig. S8 ^{1}H NMR spectrum of p-BPCDM in $CDCl_3$.

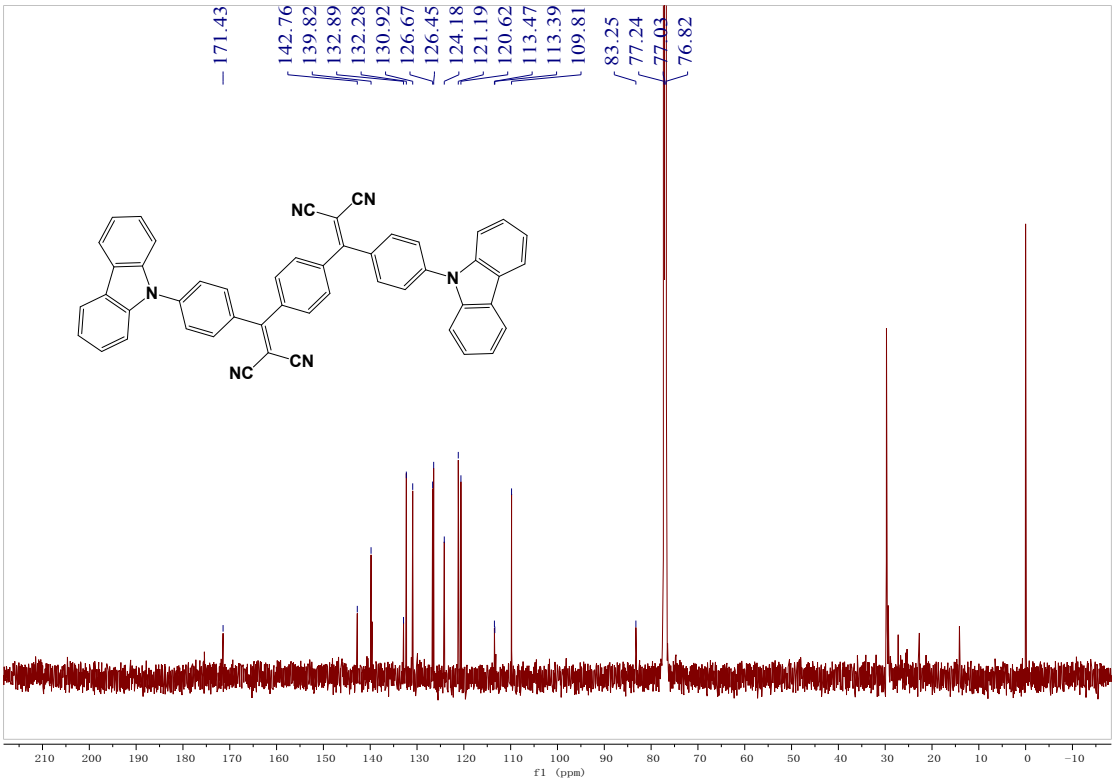

Fig. S9 ^{13}C NMR spectrum of p-BPCDM in $CDCl_3$.

Section 3. Supplement spectra

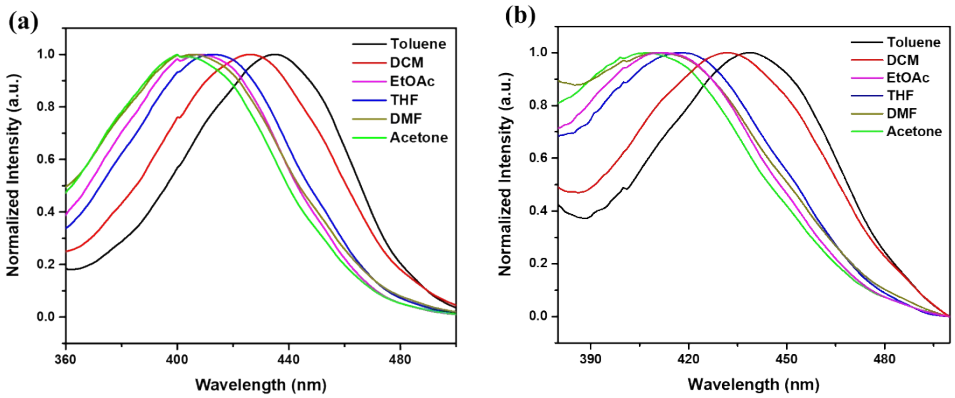

Fig. S10 The characteristic absorption peaks of normalized UV absorption spectra of m-BPCDM (a) and p-BPCDM (b) in different solvents.

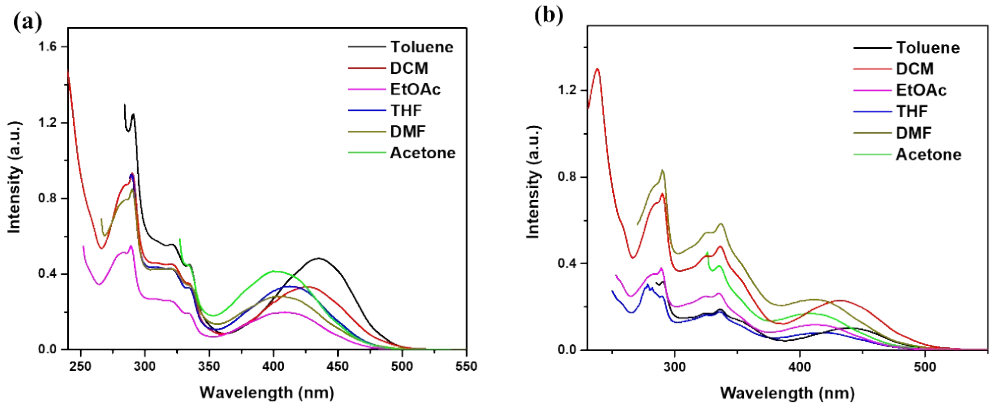

Fig. S11 (a) UV absorption spectra of m-BPCDM in different solvents. (b) UV absorption spectra of p-BPCDM in different solvents.

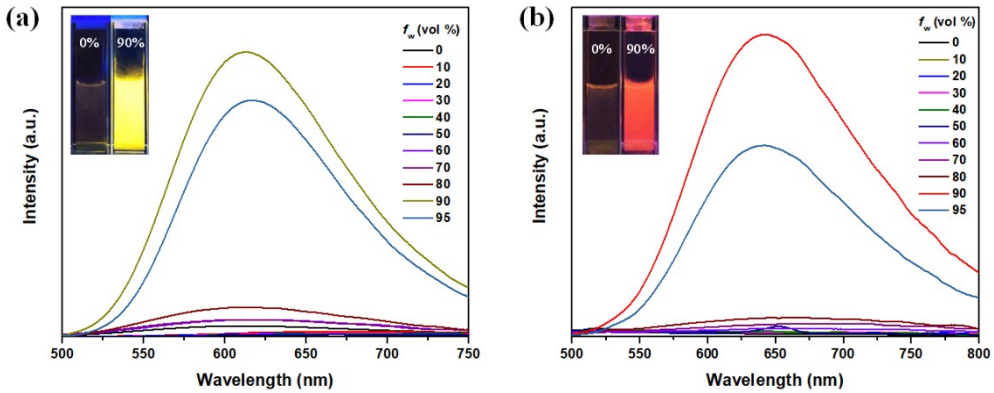

Fig. S12 PL spectra of m-BPCDM (a) and p-BPCDM (b) in THF/water mixtures with different water fractions (f_w). Concentration: 10^{-5} M (f_w= 0%); excitation wavelength: 377 nm.

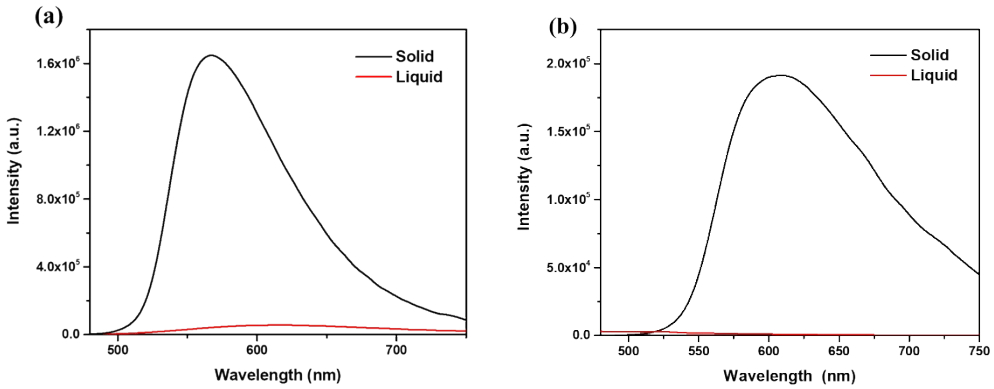

Fig. S13 PL spectra of m-BPCDM (a) and p-BPCDM (b) in solid (crystal) and in acetone solution (10^{-4} M) under UV light.

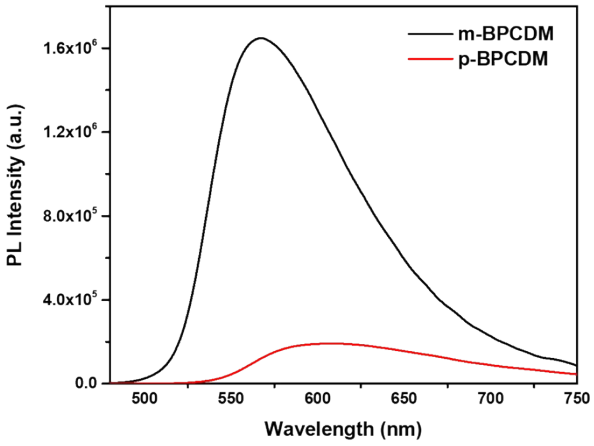

Fig. S14 PL spectra of m-BPCDM and p-BPCDM in solid (crystal) state .

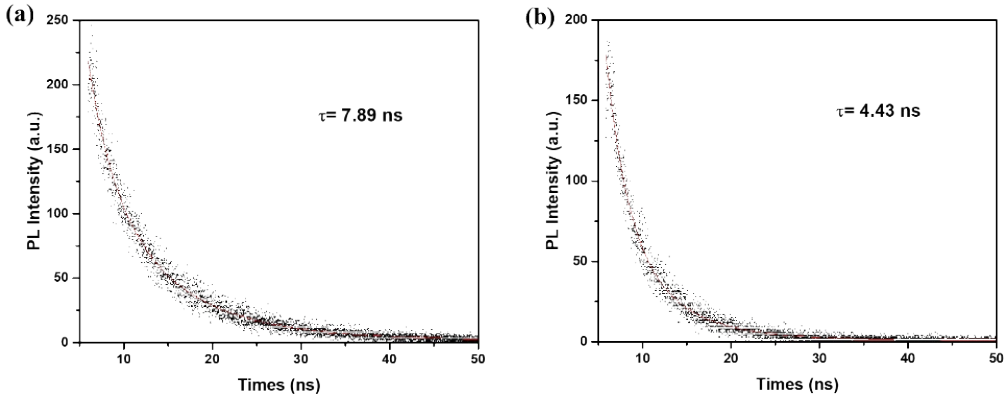

Fig. S15 Transient decay spectra of m-BPCDM (a) and p-BPCDM (b) in crystal phase, monitored at 565 nm and 609 nm respectively.

The fluorescence decay curves attained by double exponential simulation. The fitting formula is:

$$y(t)=y_0+A_1\cdot\exp(-x/t_1)+A_2\cdot\exp(-x/t_2)$$

(A_1, A_2 are the amplitude of two exponential components, and t_1, t_2 are the decay times of the two exponential components).

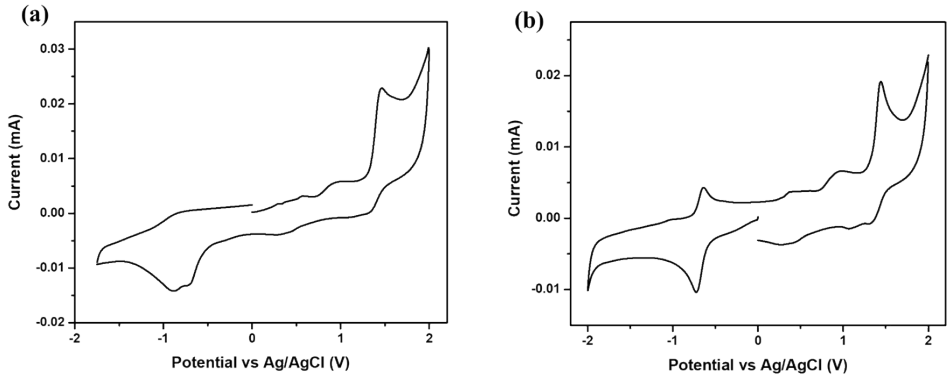

Fig. S16 (a) CV diagrams of m-BPCDM. (b) CV diagrams of p-BPCDM. Cyclic voltammetry experiments calibrated by Fc/Fc^+ with $E_{1/2}$ of 0.45 V and 0.46 V respectively. Scan rate: 100 mV/s. Concentration: 10^{-4} M. Electrolyte: 0.1 M $[(nBu)_4N]PF_6$ in CH_3CN.

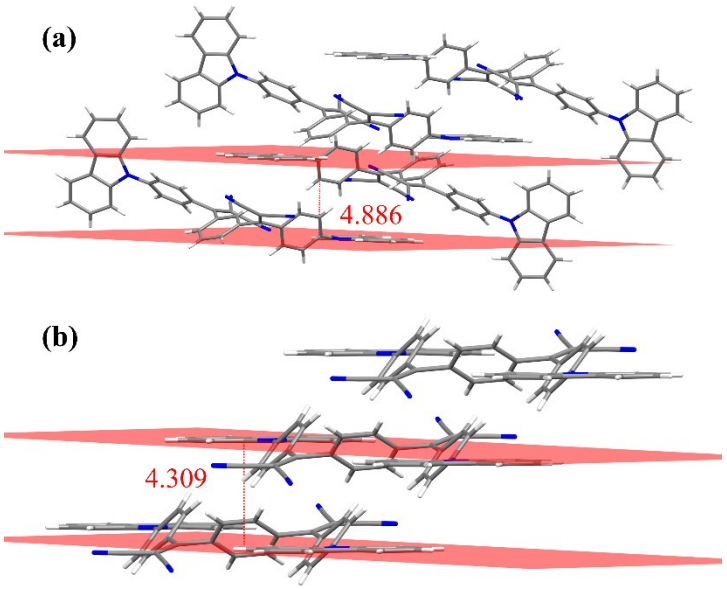

Fig. S17 The vertical distance between two packing plane of m-BPCDM (a) and p-BPCDM (b).

Section 4. X-ray Single Crystals Data

Crystals of m-BPCDM and p-BPCDM were grown in a vial with a mixture solvents of ethanol/dichloromethane/tetrahydrofuran. The vials were sealed by tin foil with several pinholes for evaporation. After that, their crystals were obtained in a few weeks, which were further analyzed by single-crystal x-ray crystallography.

A yellow block crystal picked up with paraton oil and mounted on a glass fiber was collected with a CCD area detector with graphite-monochromated Mo-Ka radiation. Reflections were collected with a Bruker SMART APEX-Ⅱ detector and processed with SAINT from Bruker. Data were corrected for Lorentz and polarization effects. Structures were solved by direct methods using SHELXTL and were refined by full-matrix least-squares on F^2 using SHELX-2014. Non-hydrogen atoms were refined with anisotropic displacement parameters during the final cycles. All hydrogen atoms of the organic molecule were placed by geometrical considerations and were added to the structure factor calculation. Solvent molecules in the crystal are highly disordered, and attempts to locate and refine these solvent peaks were unsuccessful. CCDC-1942676 and CCDC-1942677 contain the supplementary crystallographic data which can be obtained free of charge at http://www.ccdc.cam.ac.uk/conts/retrieving.html or from the Cambridge Crystallographic Data Center, 12, Union Road, Cambridge CB21EZ, UK; fax: (+44) 1223-336-033; or deposit@ccdc.cam.ac.uk).

Table S1 Photophysical properties of the m-BPCDM and p-BPCDM in different solvents (10^{-5} M).

compounds	solvents	λ_{abs} (nm)	λ_{em} (nm)	Φ (%)
m-BPCDM	Toluene	435	555	3.60
	Dichloromethane	426	571	1.38
	Ethyl acetate	408	598	0.72
	Tetrahydrofuran	413	596	0.30
	Dimethylformamide	407	605	0.15
	Acetone	402	608	0.28
p-BPCDM	Toluene	439	477	4.02
	Dichloromethane	432	493	1.14
	Ethyl acetate	413	564	0.06
	Tetrahydrofuran	418	592	0.20
	Dimethylformamide	412	594	4.22
	Acetone	407	603	0.28

Table S2 Crystallographic data of series.

Crystal	m-BPCDM	p-BPCDM
Formula	$C_{50}H_{28}N_6$	$C_{25}H_{14}N_3{\cdot}CH_2Cl_2$
Crystal system	triclinic	triclinic
Space group	P-1	P-1
a (Å)	10.7183(12)	9.681(3)
b (Å)	13.8384(16)	10.530(3)
c (Å)	14.7191(17)	12.299(3)
α (deg)	95.994(2)	65.887(5)
β (deg)	98.595(2)	70.323(5)
γ (deg)	99.932(2)	85.583(6)
V (Å^3)	2107.24	1074.8(5)
Z	2	2
μ (mm^{-1})	0.067	0.321
T (K)	200(2)	200(2)
θ_{min}-θ_{max} (deg)	1.412-27.828	1.926-28.549
R_1	0.0884	0.0691
wR_2	0.2818	0.2165
GOOF	0.993	1.048
Crystal pictures	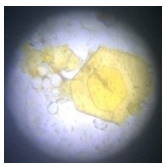	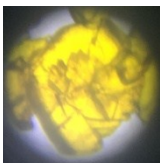
CCDC number	1942676	1942677

Section 5. Theoretical Calculation

Table S3 Molecular orbital amplitude plots of both HOMO and LUMO calculated by the B3LYP/6-31G(d) basis set.

Compound	LUMO		HOMO
m-BPCDM	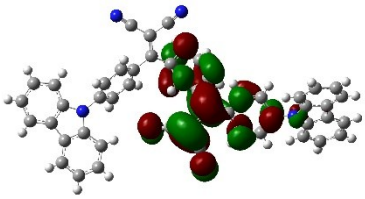	LUMO: -3.06 eV ΔE = 2.34 eV HOMO: -5.40 eV	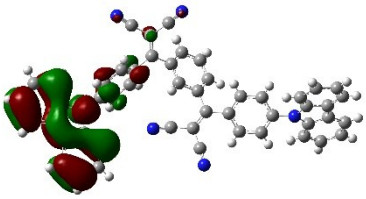
p-BPCDM	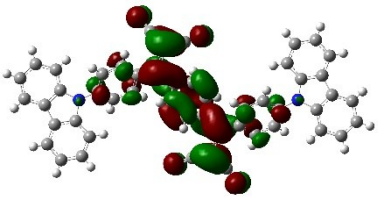	LUMO: -3.16 eV ΔE= 2.51 eV HOMO: -5.67 eV	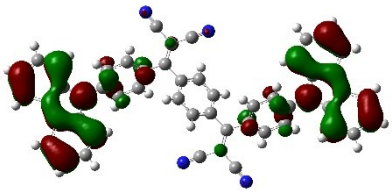
m-BPMCz	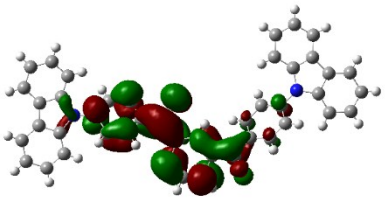	LUMO: -1.99 eV ΔE= 3.40 eV HOMO: -5.39 eV	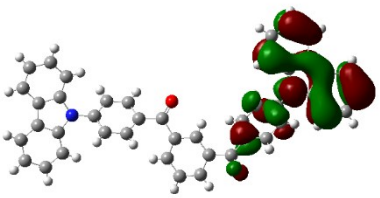
p-BPMCz	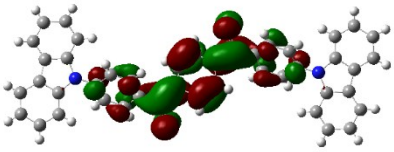	LUMO: -2.34 eV ΔE= 3.17 eV HOMO: -5.51 eV